JOURNAL OF AGRICULTURAL AND FOOD CHEMISTRY

Bioactive Constituents, Metabolites, and Functions

Oleanane- and Ursane-Type Triterpene Saponins from Centella asiatica Exhibit Neuroprotective Effects

Zhouwei Wu, Weibo Li, Jing Zhou, Xin Liu, Wang Lun, Bin Chen, Mingkui Wang, Lilian Ji, Weicheng Hu, and Fu Li

J. Agric. Food Chem., **Just Accepted Manuscript** • DOI: 10.1021/acs.jafc.0c01476 • Publication Date (Web): 05 Jun 2020

Just Accepted

is published by the American Chemical Society. 1155 Sixteenth Street N.W., Washington, DC 20036

Oleanane- and Ursane-Type Triterpene Saponins from *Centella asiatica* Exhibit Neuroprotective Effects

Zhou-Wei Wu[†,§], Wei-Bo Li[‡,§], Jing Zhou[‡], Xin Liu[∥], Lun Wang[†], Bin Chen[†], Ming-Kui Wang[†], Lilian Ji[‡], Wei-Cheng Hu*[,‡], and Fu Li*[,†]

[†]Natural Products Research Center, Chengdu Institute of Biology, Chinese Academy of Sciences, Chengdu 610041, China

[‡]Jiangsu Collaborative Innovation Center of Regional Modern Agriculture & Environmental protection/Jiangsu Key Laboratory for Eco-Agricultural Biotechnology around Hongze Lake, Huaiyin Normal University, Huaian 223300, China

[∥]Technical Center of Beijing Customs District, Beijing 100026, China

ABSTRACT: Six new pentacyclic triterpenoid saponins, centelloside F (**1**), centelloside G (**2**), 11-*oxo*-asiaticoside B (**3**), 11-*oxo*-madecassoside (**4**), 11(*β*)-methoxy asiaticoside B (**5**) and 11(*β*)-methoxy madecassoside (**6**), along with seven known ones, asiaticoside (**7**), asiaticoside B (**8**), madecassoside (**9**), centellasaponin A (**10**), isoasiaticoside (**11**), scheffoleoside A (**12**) and centelloside E (**13**), were separated from the 80% MeOH extract of the whole plant of *Centella asiatica*, which has been used as a medicinal plant and is now commercially available as a diatery supplement in many countries. Compounds **1** and **2**, **3** and **4**, **5** and **6** are three pairs of isomers with oleanane or ursane-type triterpenes as the aglycones. The chemical structures of the new triterpene saponins were fully characterized by extensive analysis of their NMR and HRESIMS data. The protective effects of

compounds **1-13** on PC12 cells induced by 6-OHDA were screened and compound **3** displayed the best neuroprotective effect with 91.75% cell viability at the concentration of 100 μM. Moreover, compound **3** also attenuated cell apoptosis and increased the mRNA expression of antioxidant enzymes including superoxide dismutase and catalase. Additionally, compound **3** activated phosphatidylinositol 3-kinase/Akt pathway including PDK1, Akt and GSK-3β. These findings suggested that triterpene saponins from *C. asiatica* were worthy of further biological research to develop new neuroprotective agents.

KEYWORDS: *Centella asiatica*, *triterpene saponins*, *neuroprotective activity*

INTRODUCTION

Centella asiatica (L.) Urban, a stoloniferous and perennial herbaceous herb belonging to the Apiaceae family, is also known as "Gotu kola" in the United States or Indian pennywort.[1] This ubiquitous species is widely growing in the moist, tropical and sub-tropical regions of Africa, Asia, and Oceania.[2] *C. asiatica* has been used for kinds of medicinal and cosmetic purposes for centuries. Preparations of this medicinal plant were traditionally used to cure various skin disorders or accelerate skin wound healing.[3,4] Nowadays, *C. asiatica* has been broadly cultivated as a salad vegetable or used as a spice and is commercially available as a diatery supplement in some countries due to its safety and effectiveness.[5] A recent *in vitro* pharmaceutical study confirmed the traditional use of this herb for management of skin disorders.[6] Also, the main compound (asiaticoside) from *C. asiatica* might be developed as a chemical agent for skin whitening or treating hyperpigmentation diseases.[7] Besides, the extract

45 of *C. asiatica* and several main individual compounds from this herb were reported to
46 have the potential to be exploited as anti-gastric ulcers drugs.[8] The *C. asiatica*
47 methanol extract could protect mouse brain from paracetamol-induced stress because
48 of its anti-oxidant and anti-inflammatory activities and the principal components
49 (asiaticoside and madecassoside) were considered as the active subtances.[9]
50 Asiaticoside from *C. asiatica* can also attenuate RANKL-induced osteoclasogenesis
51 and thus might play a role in treating osteoclast-related osteolytic bone diseases.[10]
52 Neurodegenerative diseases are affecting more and more middle-aged and elderly
53 people throughout the world. Developing neuroprotective drugs from natural
54 resources is a promising research direction. Neuroprotective effects of the extract of *C.*
55 *asiatica* had been investigated and the active subtances were thought to be associated
56 with triterpene saponins and caffeoylquinic acids in the herb.[8] *C. asiatica* is rich in
57 triterpene saponins chiefly composed of oleanolic and ursolic acids based glycosides,
58 accounting for around 8% of the dry weight of this herb.[11-15] However, previous
59 pharmaceutical researches mainly focused on the neuroprotective actions of the crude
60 extract and several main components from *C. asiatica*.[8] It is necessary to discover
61 more chemical individuals from *C. asiatica* and evaluate their neuroprotective
62 functions, allowing a better exploitation of this valuable resource. As caffeoylquinic
63 acids from *C. asiatica* were also widely present in many other plants and their
64 chemical structures were relatively fixed, we focused on the investigation of triterpene
65 saponins from this plant. An HPLC-HR-ESI-MS experiment was performed to
66 analyze the chemical profile of the crude triterpene saponins in *C. asiatica* and several

67 unreported compounds were detected (see Supporting Information). Herein, the
68 detailed isolation and structure determination of thirteen triterpene saponins including
69 six new ones, along with their neuroprotective effects, were described.

70 ■ **MATERIALS AND METHODS**

71 **Materials and Chemicals.** *C. asiatica* were purchased from Lotus Pond Chinese
72 Herbal Medicine Market, Sichuan province, China. The plant identification was
73 verified by Professor Wei-Kai Bao of Chengdu Institute of Biology, Chinese
74 Academy of Sciences. A voucher specimen (JXC-100) was deposited in the
75 herbarium of the same department. Silica gel (100–200 mesh) was bought from
76 Qingdao Haiyang Chemical Group Co. Ltd. (Qingdao, China). Standard sugars
77 (L-rhamnose, D-glucose and L-glucose), 6-Hydroxydopamine hydrobromide
78 (6-OHDA) and 3-4,5-dimethylthiazol-2-yl)-2,5-diphenyltetrazolium bromide (MTT)
79 were obtained from Sigma-Aldrich (St. Louis, MO, USA). The fetal bovine serum
80 (FBS) was purchased from Corning (Medford, MA, USA). Penicillin–streptomycin
81 solution was obtained from Invitrogen-Gibco (Carlsbad, CA, USA). Protease and
82 phosphatase inhibitors cocktail tablets were from Roche (Mannheim, Germany).
83 Phosphate buffered saline (PBS) tables was bought from Amresco (Solon, OH, USA).
84 Goat anti-rabbit lgG H&L (HRP) was purchased from abcam (Cambridge, MA, USA).
85 Caspase-3, PARP, phospho-PDK1, PDK1, phospho-GSK-3β, GSK-3β, phospho-Akt,
86 and Akt were maintained from Cell Signaling Technology (Beverly, MA, USA).
87 DAPI containing mounting medium were obtained from Solarbio Life Sciences
88 (Shanghai, China). All cell culture suppliers were bought from Coster (Cambridge,

89 MA). Acetonitrile and methanol (HPLC grade), petroleum ether (analytical grade),
90 methanol, ethyl acetate and dichloromethane were bought from KeLong (Chengdu,
91 China). Pyridine-d5 was obtained from CIL Co. (YRTC, China). The stock solutions
92 of compounds were prepared in DMSO to 100 mM and the final concentration of
93 DMSO was not in excess of 0.1% at any treatment.

94 **General Experimental Procedures.** UV spectra, infrared (IR) spectra and optical
95 rotations were recorded on a PerkinElmer lambda 35 UV/vis spectrophotometer, a
96 PerkinElmer 1725X-FT spectrometer and a PerkinElmer 341 polarimeter, respectively.
97 1D and 2D nuclear magnetic resonance (NMR) spectra were acquired at 296 K on a
98 Bruker Avance-400 spectrometer in C_5D_5N with TMS as internal standard. An
99 HPLC-MS experiment was performed on a Waters Vion IMS Q-TOF spectrometer
100 (Waters, UK), connected to Waters HPLC system (Waters, UK). The crude samples
101 were separated on a Minxitech CG-C18 column (4.6 mm × 250 mm, 5.0 μm). 0.1%
102 formic acid in water (A) and acetonitrile (B) were used as the mobile phase and a
103 gradient elution program was as follows: 0 min, 25% B; 10 min, 25% B; 50 min, 30%
104 B; 60 min, 30% B. High resolution electrospray ionization mass spectrometry
105 (HR-ESI-MS) data were generated on a LTQ Orbitrap XL mass spectrometer
106 (Thermo Fisher Scientific, San Jose, CA, USA). LabAlliance Series III equipped with
107 a model 201 (SSI) detector (Alltech, California, USA) and a SinoChrom ODS-BP
108 C18 column (4.6 mm × 250 mm, 5 μm, Elite, Dalian, China) was used to analyze the
109 sugar derivatives. Preparative and semipreparative HPLC separations were carried out
110 on a CXTH apparatus with a UV3000 detector (Beijing Innovation Technology Co.

111 Ltd., Beijing, China) equipped with Unisil-10-120-C18 (250 × 100 mm, 10 μm) and
112 Unisil-10-120-C18 (250 × 30 mm, 10 μm) columns (Nanomicro Technology Co. Ltd.,
113 Suzhou, China), respectively. The flowrates for preparative and semipreparative
114 purifications were 200 mL/min and 20 mL/min, respectively.

115 **Extraction and Isolation.** The air-dried whole plants (aerial parts and roots) of *C.*
116 *asiatica* (50.0 Kg) was smashed and extracted with 80% MeOH (120 L) at 60 °C
117 three times (24 h each time). The combined extract solutions were concentrated under
118 reduced pressure and the resultant dark residue was suspended in distilled water and
119 extracted with CH_2Cl_2 and *n*-BuOH, successively. The dried *n*-BuOH extract (2.0 kg)
120 was dissolved in MeOH and mixed with 4.0 kg of silica gel, which was dried under
121 reduced pressure and then fractionated over a silica gel column (1000 mm × 300 mm)
122 eluted with a trinary gradient solvent system of H_2O saturated MeOH/CH_2Cl_2 (10:1,
123 8:1, 6:1, 4:1, 2:1, 1:1) to give ten fractions (Fractions A-J). Fraction F was separated
124 by preparative HPLC using MeOH-H_2O (200 mL/min, 57:42, v/v) to afford five
125 subfractions (subfractions F1-F5). Further purification of subfraction F4 by
126 semipreparative HPLC using CH_3CN-H_2O (20 mL/min, 25/75, v/v) as eluent afforded
127 compounds **10** (38.0 mg, t_R 19.1 min), **11** (270.1 mg, t_R 23.6 min) and **13** (38.0 mg, t_R
128 25.8 min). The subfraction F5 was applied to preparative HPLC using CH_3CN-H_2O
129 with 4mmol/L β-cyclodextrin (200 mL/min, 25/75, v/v) as eluent to give compounds
130 **7** (56.1 g, t_R 26.9 min) and **12** (750.0 mg, t_R 17.9 min). Fraction H was firstly purified
131 by preparative HPLC with MeOH-H_2O (200 mL/min, 57:42, v/v) as mobile phase to
132 yield five subfractions (subfractions H1-H5). Semipreparative HPLC separation of

133 subfraction H2 with CH_3CN-H_2O containing 4mmol/L β-cyclodextrin (20 mL/min,
134 20/80, v/v) as eluent afforded compounds **3** (214.3 mg, t_R 22.4 min) and **4** (82.1 mg,
135 t_R 16.9 min). Compounds **5** (170.4 mg, t_R 30.7 min) and **6** (43.2 mg, t_R 24.2 min) were
136 obtained from subfraction H3 by semipreparative HPLC using CH_3CN-H_2O with
137 4mmol/L β-cyclodextrin (20 mL/min, 23/77, v/v) as eluent. Semipreparative HPLC
138 purification of subfraction H4 with CH_3CN-H_2O containing 4mmol/L β-cyclodextrin
139 (20 mL/min, 25/75, v/v) as eluent gave compounds **1** (259.7 mg, t_R 20.5 min) and **2**
140 (60.4 mg, t_R 16.7 min). Large-scale preparation of compounds **8** (67.3 g, t_R 27.6 min)
141 and **9** (143.7 g, t_R 21.4 min) from subfraction H5 was achieved by repeated
142 preparative HPLC using CH_3CN-H_2O with 4mmol/L β-cyclodextrin (200 mL/min,
143 25/75, v/v) as eluent. The mixtures of the isolated compounds and β-cyclodextrin
144 were separated by a short column with silica gel as stationary phase and
145 MeOH-CH_2Cl_2-H_2O (10:30:1, v/v/v) as mobile phase.

146 **Structural Identification of the Sugar Residues.** Compounds **1-6** (each 3 mg)
147 were mixed and dissolved in 2% H_2SO_4 solution (4 mL) and heated at 100 °C for 12 h.
148 The resultant solution was cooled to room temperature and then extracted with EtOAc
149 three times (each 5 mL) to remove the nonpolar aglycones. The remaining H_2O layer
150 was neutralized to pH = 7 with aqueous solution of $Ba(OH)_2$, filtered, and identified
151 using TLC with authentic samples. The absolute configuration of sugars was
152 determined by the method previouly reported.[16] D-glucose and L-rhamnose were
153 detected in the hydrolysate of compounds **1-6** by comparison of the HPLC retention
154 times of their derivatives with those of the authentic standards derivatized in the same

155 way.

156 *Centelloside F (**1**)*. White amorphous powder; $[\alpha]_D^{20}$ +24.3 (c 0.15 , MeOH); UV
157 (MeOH) λ_{max} 284; IR ν_{max} (KBr) 3382, 2934, 1733, 1669, 1383, 1051 cm^{-1};
158 HRESIMS *m/z* 995.4822 $[M+Na]^+$, (calcd for $C_{48}H_{76}O_{20}Na^+$, 995.4822); ^1H and ^{13}C
159 NMR data are shown in Tables 1 and 2.

160 *Centelloside G (**2**)*. White amorphous powder; $[\alpha]_D^{20}$ +28.8 (c 0.11 , MeOH); UV
161 (MeOH) λ_{max} 283; IR ν_{max} (KBr) 3369, 2930, 1733, 1699, 1602, 1388, 1060 cm^{-1};
162 HRESIMS *m/z* 995.4825 $[M+Na]^+$, (calcd for $C_{48}H_{76}O_{20}Na^+$, 995.4822); ^1H and ^{13}C
163 NMR data are shown in Tables 1 and 2.

164 *11-oxo-asiaticoside B (**3**)*. White amorphous powder; $[\alpha]_D^{20}$ +11.3 (c 0.11, MeOH);
165 UV (MeOH) λ_{max} 253; IR ν_{max} (KBr) 3323, 2942, 1732, 1645, 1262, 1024 cm^{-1};
166 HRESIMS *m/z* 989.4962 $[M+H]^+$ (calcd for $C_{48}H_{77}O_{21}^+$, 989.4952); ^1H and ^{13}C NMR
167 data are shown in Tables 1 and 2.

168 *11-oxo-madecassoside (**4**)*. White, amorphous powder; $[\alpha]_D^{20}$ +2.9 (c 0.34, MeOH);
169 UV (MeOH) λ_{max} 252; IR (KBr) ν_{max} 3424, 2922, 1740, 1653, 1242, 1024 cm^{-1};
170 HRESIMS *m/z* 989.4960 $[M+H]^+$ (calcd for $C_{48}H_{77}O_{21}^+$, 989.4952); ^1H and ^{13}C NMR
171 data are shown in Tables 1 and 2.

172 *11(β)-methoxy asiaticoside B (**5**)*. White amorphous powder; $[\alpha]_D^{20}$ -33.3 (c 0.11,
173 MeOH); IR ν_{max} (KBr) 3355, 2941, 1746, 1630, 1434, 1062 cm^{-1}; HRESIMS *m/z*
174 1027.5087 $[M+Na]^+$ (calcd for $C_{49}H_{80}O_{21}Na^+$, 1027.5084); ^1H and ^{13}C NMR data are
175 shown in Tables 1 and 3.

176 *11(β)-methoxy madecassoside (**6**)*. White amorphous powder; $[\alpha]_D^{20}$ -45.0 (c 0.11,
177 MeOH); IR (KBr) ν_{max} 3391, 2941, 1750, 1669, 1395, 1072 cm^{-1}; HRESIMS *m/z*
178 1027.5104 $[M+Na]^+$ (calcd for $C_{49}H_{80}O_{21}Na^+$, 1027.5084); ^1H and ^{13}C NMR data are

179 shown in Tables 1 and 3.

180 **Cell Culture.** The cell culture of neuronal differentiated rat pheochromocytoma
181 PC12 was performed as previous mentioned.[17] Briefly, PC12 cells were maintained in
182 DMEM containging 5% (v/v) horse serum (HS), 10% (v/v) FBS, 100 U/mL penicillin
183 and 100 μg/mL streptomycin at 37°C under 5% CO_2 in a humidified CO_2 incubator
184 (Heracell 150i, Thermo Fisher Scientific, Waltham, MA, USA).

185 **Cell Viability.** Briefly, PC12 cells were seeded at 3×10^5 cells/mL on 96-well cell
186 culture plates for overnight. The cells were pre-treated different samples with the final
187 concentration of 100 μM for 30 min and then exposed to 250 μM 6-OHDA for 24 h.
188 The cytoprotective effect of different samples on PC12 cells were measured using a
189 conventional MTT assay described previously.[18]

190 **Reverse-Transcribed and Quantitative PCR (RT-qPCR).** PC12 cells were
191 pretreated with 50 or 100 μM compound **3** for 30 min, and then exposed to 6-OHDA
192 for 6 h. Total RNA was extracted using TRIzol reagent according to the
193 manufacturer's protocol. The purity of RNA was determined by the NanoDrop One
194 (Thermo Scientific, CN, US). cDNA was prepared from two micrograms of RNA in a
195 reaction volume of 20 μl with RevertAid First Strand cDNA Synthesis Kit. The
196 primer sequences used in the PCRs are listed in Table **4**. Semi-quantitative PCR
197 amplifications were performed with 2 x Es Taq MasterMix (CWBIO, China) using
198 Bio-Rad T100 Thermal Cycle (Bio-Rad, USA) and the PCR products were
199 electrophoresed on 1.5% agarose gels with 0.005% Golden View.

200 **Western Blot.** PC12 cells were pretreated with 50 or 100 μM compound **3** for 30
201 min, and then exposed to 6-OHDA for 6 h. The cells were washed twice with cold
202 PBS and the total nuclear proteins were lysed to release using the commercial kits.
203 The protein bands were visualized using an ECL kit (CWBIO, China) and visualized
204 using Tannon 5200 Multi imaging system (Shanghai, China).

205 **Statistical Analysis.** Data were presented as the mean ± standard deviation (SD).
206 The significance was analyzed by one-way analysis of variance (ANOVA) followed
207 by Duncan's test for multi-group comparison. *p* values of less than 0.05 were
208 considered significant.

209 ■ **RESULTS AND DISSCUSION**

210 **Structural Elucidation.** Compound **1**, a white amorphous powder, had the
211 molecular formula of $C_{48}H_{76}O_{20}$ according to its HRESIMS at *m/z* 995.4822 $[M+Na]^+$
212 in positive ion mode. The IR spectrum displayed characteristic absorptions for
213 hydroxyl (3382cm^{-1}), carbonyl (1733cm^{-1}) and olefinic (1669cm^{-1}) groups. The ^{13}C
214 and ^{1}H NMR data (Tables 1 and 2) of compound **1** indicated the existance of seven
215 methyl groups at δ_H 0.82 (s) / δ_C 23.7, δ_H 0.82 (s) / δ_C 33.1, δ_H 1.15 (s) / δ_C 20.4, δ_H
216 1.66 (d, J = 5.8 Hz) / δ_C 18.6, δ_H 1.71 (s) / δ_C 16.1, δ_H 1.94 (s) / δ_C 23.0, and δ_H 2.04 (s)
217 / δ_C 30.4, three oxymethylenes at δ_H 3.99 (m), 4.36 (m) / δ_C 66.5, δ_H 4.28 (m), 4.65 (m)
218 / δ_C 69.8, δ_H 4.02 (m), 4.13 (m) / δ_C 61.3, and two olefinic methines at δ_H 5.75 (d, J =
219 5.2 Hz) / δ_C 121.5, δ_H 6.00 (d, J = 5.2 Hz) / δ_C 116.4. The ^{13}C and ^{1}H NMR data
220 (Tables 1 and 2) of compound **1** also demonstrated signals for three anomeric protons
221 and carbons at δ_H 4.96 (d, J = 7.0 Hz) / δ_C 104.9, δ_H 5.83 (br s) / δ_C 102.6, δ_H 6.18 (d, J

222 = 7.5 Hz) / δ_C 95.8. The absolute configurations of the sugar residues were determined
223 to be D-glucose and L-rhamnose by the method previously reported.[16] The ^{1}H and ^{13}C
224 NMR spectra of **1** resembled those of asiaticoside B (**8**) except for the presence of two
225 double bonds in **1**. The absorption band at 284 nm in the UV spectrum indicated these
226 two double bonds were conjugated,[19] which were further confirmed to be located at
227 $\Delta^{9,11}$ and $\Delta^{12,13}$ due to the important HMBC correlations from H-11 (δ_H 5.75) to C-8
228 (δ_C 42.0), C-9 (δ_C 155.5), C-10 (δ_C 39.9), C-12 (δ_C 116.4) and C-13 (δ_C 145.1), H-12
229 (δ_H 6.00) to C-9 (δ_C 155.5), C-14 (δ_C 42.5) and C-18 (δ_C 40.2), H-25 (δ_H 2.04) to C-9
230 (δ_C 155.5), H-26 (δ_H 1.94) to C-9 (δ_C 155.5), and H-27 (δ_H 1.15) to C-13 (δ_C 145.1)
231 (Figure 2). The relatively large coupling constant J_{23} = 9.4 Hz of the two methine
232 protons at C-2 and C-3, along with the chemical shifts of C-2 (δ_C 69.8) and C-3 (δ_C
233 78.2), confirmed the *equatorial* position of the hydroxyl groups at C-2 and C-3 in
234 comparison with the corresponding data for 2β,3α,23-trihydroxyurs-12-en-28-oic acid
235 [δ_C values for C-2 (66.6) and C-3 (78.6)] and methyl
236 2α,3α,24-trihydroxyurs-12-en-28-oate [δ_C values for C-2 (66.6) and C-3 (73.3)].[20,21]
237 This was further verified by the correlation between H-2 (δ_H 4.49) and H-25 (δ_H 2.04)
238 in NOESY spectrum. Meanwhile, the chemical shifts of C-2 (δ_C 69.8) and C-3 (δ_C
239 78.2) were quite different from those reported for scheffursoside F [δ_C values for C-3
240 (85.7) and C-24 (65.7)],[22] suggesting the presence of a hydroxyl group at C-23. This
241 was ulteriorly verified by an obvious cross peak between H-24 (δ_H 1.71) and H-25 (δ_H
242 2.04) in the NOESY spectrum. A cross peak between H-6 (δ_H 5.09) and H-27 (δ_H 1.15)
243 was observed in the NOESY spectrum, indicating the 6-OH was β-oriented. The

244 HMBC cross peaks between H-1 (δ_H 6.18) of Glc-I and C-28 (δ_C 176.8) of the
245 aglycone, H-1 (δ_H 4.96) of Glc-II and C-6 (δ_C 69.8) of Glc-I, H-1 (δ_H 5.83) of Rha and
246 C-4 (δ_C 78.6) of Glc-II demonstrated the sugar sequence and linkage positions. The
247 structure of **1** was defined as 2α,3β,6β,23-tetrahydroxyolean-9,12-diene-28-oic acid
248 28-O-α-L-rhamnopyranosyl (1→4)-β-D-glucopyranosyl(1→6)-β-D-glucopyranoside
249 (Figure 1) and named centelloside F.

250 The molecular formula of compound **2**, $C_{48}H_{76}O_{20}$, was deduced from the
251 HRESIMS peak at *m/z* 995.4825 $[M+Na]^+$. The ^{13}C and ^1H NMR data (Tables 1 and
252 2) of compound **2** resembled those of compound **1** for rings A-D and the sugar
253 residues. Comparison of the differing ^{13}C NMR data for ring E between compounds **1**
254 and **2** with those between centellasaponin G and centellasaponin H evidenced that **2**
255 possessed an ursane-type aglycone rather than an oleanane-type aglycone in **1**,[12]
256 which was further verified by the cross-peaks between H-29 (δ_H 0.90) and C-18 (δ_C
257 51.6), H-30 (δ_H 0.84) and C-21 (δ_C 30.8) in the HMBC spectrum. The above evidence,
258 along with the DEPT and HSQC data, defined the structure of **2** as
259 2α,3β,6β,23-tetrahydroxyurs-9,12-diene-28-oic acid 28-O-α-L-rhamnopyranosyl
260 (1→4)-β-D-glucopyranosyl(1→6)-β-D-glucopyranoside, named centelloside G.

261 Compound **3** was obtained as a white powder, and the peak at *m/z* 989.4962
262 $[M+H]^+$ in the HRESIMS indicated its molecular formula as $C_{48}H_{76}O_{21}$. The ^{13}C and
263 ^1H NMR data (Tables 1 and 2) of compound **3** closely resembled those of asiaticoside
264 B (**8**) except that a methylene group in **8** was replaced by a carbonyl group in **3**. The
265 absorption band at 253 nm in the UV spectrum and the chemical shift of C-13

266 downfield shifted from around δ_C 143.4 to δ_C 169.2 indicated the carbonyl group was
267 probably located at C-11,[23] which was further supported by the HMBC cross peaks
268 between H-9 (δ_H 2.86) and C-11 (δ_C 200.6), H-12 (δ_H 6.00) and C-9 (δ_C 63.1), C-14
269 (δ_C 44.8) and C-18 (δ_C 42.3). By detailed analysis of the DEPT, ^{1}H-^{1}H COSY, HSQC,
270 NOESY and HMBC data, **3** was ulteriorly identified as 2α,3β,6β,23-
271 tetrahydroxy-11-oxo-olean-12-ene-28-oic acid 28-O-α-L-rhamnopyranosyl
272 (1→4)-β-D-glucopyranosyl(1→6)-β-D-glucopyranoside, named 11-*oxo*-asiaticoside
273 B.

274 Compound **4**, a white powder, showed an HRESIMS peak at *m/z* 989.4960
275 $[M+H]^+$, suggesting a molecular formula of $C_{48}H_{76}O_{21}$. By comparison of the ^{13}C and
276 ^{1}H NMR data (Tables 1 and 2) of **4** with those of **3**, it was easy to conclude that the
277 differences between these two compounds were the same as those between
278 compounds **1** and **2**, indicating compound **4** bore a ursane-type aglycone. Extensive
279 analysis of the DEPT, ^{1}H-^{1}H COSY, HSQC, NOESY and HMBC spectra further
280 confirmed the structure of **4** as 2α,3β,6β,23- tetrahydroxy-11-oxo-urs-12-ene-28-oic
281 acid 28-O-α-L-rhamnopyranosyl (1→4)-β-D-glucopyranosyl
282 (1→6)-β-D-glucopyranoside, named 11-*oxo*-madecassoside.

283 Compound **5**, a white amorphous powder, had the molecular formula of $C_{49}H_{80}O_{21}$
284 deduced from its HRESIMS peak at *m/z* 1027.5087 $[M+Na]^+$. The ^{13}C and ^{1}H NMR
285 data (Tables 1 and 3) of **5** were quite similar to those of asiaticoside B (**8**) except for
286 the occurrence of a methoxy group δ_H 3.30 (s) / δ_C 54.3 in **5**, which was located at
287 C-11 according to the HMBC correlations between H-9 (δ_H 2.25) and C-11 (δ_C 76.4),

288 H-12 (δ_H 5.48) and C-11 (δ_C 76.4), OCH_3 (δ_H 3.30) and C-11 (δ_C 76.4). The NOESY
289 correlations of the OCH_3 (δ_H 3.30) with H-25 (δ_H 1.89), H-26 (δ_H 1.75) and H-1β (δ_H
290 2.75) strongly implied that the OCH_3 group was in β orientation. In combination with
291 the DEPT ^{1}H-^{1}H COSY, NOESY and HSQC data, the chemical structure of **5** was
292 defined as 2α,3β,6β,23-tetrahydroxy-11β-methoxy-olean- 12-ene-28-oic acid
293 28-O-α-L-rhamnopyranosyl (1→4)-β-D-glucopyranosyl(1→6) -β-D-glucopyranoside,
294 named 11(*β*)-methoxy asiaticoside B.

295 The molecular formula of compound **6** was defined as $C_{49}H_{80}O_{21}$ based on the
296 peak at *m/z* 1027.5104 $[M+Na]^+$ in the HRESIMS. By comparison of the ^{13}C and ^{1}H
297 NMR data (Tables 1 and 3) of **6** with those of **5**, it was obvious that these two
298 compounds shared the same rings A-D and only differed in ring E. The above
299 1D-NMR data, along with the DEPT, HSQC and HMBC data, supported the structure
300 of **6** as 2α,3β,6β,23-tetrahydroxy-11β-methoxy-urs-12-ene-28-oic acid
301 28-O-α-L-rhamnopyranosyl(1→4)-β-D-glucopyranosyl(1→6)-β-D-glucopyranoside
302 and named as 11(*β*)-methoxy madecassoside.

303 The seven known compounds **7-13** were identified as asiaticoside (**7**),[24]
304 asiaticoside B (**8**),[24] madecassoside (**9**),[24] centellasaponin A (**10**),[15] isoasiaticoside
305 (**11**),[25] scheffoleoside A (**12**)[22] and centelloside E (**13**)[26] respectively, based on
306 comparison of their spectral data with those reported in the literature.

307 **Effects of compounds 1-13 and 6-OHDA on PC12 cell viability.** To date, there
308 is no safe and effective cure for Parkinson's disease (PD). Surgical and
309 pharmacological treatments alleviate the symptoms of patients to some extent, but

310 with severe side effects on normal tissues. Consequently, a suitable natural candidate
311 for halting or retarding the progress of PD is urgently needed.[27,28] Since the discovery
312 that 6-OHDA effectively causes dopamine neuron degeneration, this neurotoxin has
313 been comprehensively used to generate a cell model of PD.[29] As shown in Table 5,
314 treatment with 250 μM 6-OHDA resulted in a 40.96% loss of viability, and therefore
315 250 μM 6-OHDA was deemed as an appropriate concentration for use in the
316 following experiments. Moreover, compounds **1-13** did not affect the cell viability at
317 100 μM (data not shown). Compounds **1**, **5**, **6** and **10** displayed weak activities, while
318 compounds **2**, **4**, **12** and **13** presented moderate activities. It was interesting that the
319 three main compounds (**7**, **8** and **9**) in *C. asiatica* all showed good activities,
320 suggesting this medicinal plant was an ideal natural resource for treating related
321 diseases. These results suggested that the neuroprotective effect of these individual
322 compounds from *C. asiatica* was not attributable to an effect on the cell division.
323 Madecassoside (compound **9**), a well-known neuroprotective agent,[30] offered smaller
324 protection than that of compound **3**, which was therefore selected for further
325 investigation of inhibitory effect on 6-OHDA-induced toxicity in PC12 cells and the
326 possible mechanism.

327 **Effect of compound 3 on 6-OHDA-induced apoptosis.** Caspase-dependent
328 apoptosis plays crucial roles in the regulation of apoptosis transduction pathways,
329 especially in the mitochondrial pathway.[31] The apoptotic stimuli to mitochondria
330 promotes the formation of the apoptosome, leading to the activation of caspase-3,
331 which serves as executioner molecule in cleaving downstream substrate proteins

332 including poly (ADP-ribose) polymerase (PARP), resulting in triggering
333 chromosomal DNA fragmentation apoptosis and neuronal death.[32] To gain insight
334 into the molecular effector pathway of cytoprotective of compound **3** on
335 6-OHDA-induced cytotoxicity, we first analyzed whether caspases-3 and pro-PARP
336 involved as down-stream effectors in 6-OHDA-mediated apoptosis. The expression of
337 apoptosis-related proteins was assayed by western blot (Figure 3). In 6-OHDA-treated
338 PC12 cells, caspase-3 was activated, resulting in the cleavage of pro-PARP.
339 Conversely, activation of these pro-apoptotic factors was attenuated by the compound
340 **3**. These results suggest that compound **3** exerts its neuroprotective action by
341 inhibiting the activation of caspase-3 expression.

342 **Effect of compound 3 on 6-OHDA induced mRNA expression of antioxidant**
343 **enzymes.** In addition to apoptosis, oxidative stress also causes alterations in proteins,
344 lipids, DNA, and glycogens. These alterations occur as a result of free-radical
345 accumulation and poor efficacy of antioxidant enzymes, such as superoxide dismutase
346 (SOD), catalase (CAT), and glutathione peroxidase (GSH-Px).[33,34] Oxygen free
347 radical reactions and lipid peroxidation play important roles in the metabolic process;
348 under physiological conditions, the two are in a state of coordination and dynamic
349 equilibrium, maintaining many physiological and biochemical reactions, and immune
350 responses in the body.[35,36] To investigate whether suppression of ROS accumulation
351 contributed to prevention of apoptosis, the expression levels of CAT and SOD were
352 measured in 6-OHDA-induced PC12 cells (Figure 4). The results show that
353 compound 3 ameliorated antioxidant enzyme expression levels, implying that the

354 neuroprotective effect of compound **3** is mediated by attenuating oxidative stress.

355 **Effects of compound 3 on 6-OHDA induced PI3K/Akt/GSK-3β signaling**
356 **pathway.** Previous studies have demonstrated that cell proliferation, progression, and
357 apoptosis are linked with PI3K/Akt/GSK-3β pathways.[37-39] The PI3K/Akt pathway
358 regulates downstream genes such as the apoptosis gene Bax and the nuclear
359 transcription factor NF-κB, thereby regulating cell apoptosis to achieve
360 neuroprotective effects.[40,41] PI3K, a member of the phosphatidylinositol 3-kinase
361 family, catalyzes the generation of lipid second messengers.[42] PI3K is a heterologous
362 polymer structure composed of a catalytic subunit and a receptor-binding regulatory
363 subunit, p85. Phosphoryl diphosphate inositol (PIP2) can be phosphorylated into
364 inositol triphosphate (PIP3) after activation, which is the second messenger of
365 multiple peptide hormones and membrane receptors.[43] Once Ser473 is phosphorylated,
366 Akt transforms the downstream gene CREB into phosphorylated CREB, which is
367 involved in cell differentiation, proliferation, survival, and apoptosis.[44] Increasing
368 evidence indicates that PI3K/Akt/GSK-3β signaling plays a leading role in the
369 prevention and treatment of cell degeneration.[45-47] To explore the underlying
370 neuroprotective mechanism, proteins related to the PI3K/Akt/GSK-3β pathway was
371 measured. As shown in Figure 5, inhibition of p-forms of PDK1, Akt, and GSK-3β
372 occurred following 6-OHDA treatment, but levels of p-AKT, p-PDK1, and p-GSK-3β
373 were enhanced by pretreatment with compound **3**, indicating that PI3K/Akt/GSK-3β
374 may mediate the neurological protective effects of compound **3** and be associated with
375 pathogenesis in PD.

A detailed phytochemical investigation on the *n*-BuOH fraction of 80% methanol extract of *C. asiatica* was carried out to afford six new triterpene saponins, which are three pairs of isomers bearing oleanane or ursane type derivatives as the aglycones. Oleanolic and ursolic pentacyclic triterpenoid isomers often coexist in many plants due to their same biosynthesis pathways. It was reported that hydrophilic β-cyclodextrin derivatives could well improve the separation efficiency of oleanolic and ursolic pentacyclic triterpenoids isomers when they carried big hydrophilic groups in analytical reversed-phase HPLC.[48] To the best of our knowledge, this is the first report that shows β-cyclodextrin can also be used to well obtain large-scale individual compounds from mixtures of oleanolic and ursolic pentacyclic triterpenoids isomers. Moreover, it was demonstrated that compound **3** suppressed 6-OHDA-induced oxidative stress and apoptosis, and this was accompanied with PI3K/AKT/GSK/3β signaling pathway. The preparation of compound **3** on a gram-scale is in progress and its overall *in vivo* neuroprotective effect will be investigated in the future.

ASSOCIATED CONTENT

Supporting Information

The Supporting Information is available free of charge on the ACS Publications website.

UV, IR, HRESIMS, NMR spectra of compounds **1**–**6**.

AUTHOR INFORMATION

Corresponding Authors

398 * Telephone/Fax: +86-517-83525992. E-mail: hu_weicheng@163.com (W.-C. H.).

399 Telephone/Fax: +86-28-82890820. E-mail: lifu@cib.ac.cn (F. L.).

400 **Funding**

401 This research was financially supported by Natural Science Foundation of the Higher

402 Education Institutions of Jiangsu Province (17KJA550001).

403 **Notes**

404 The authors declare no competing financial interest.

405 [§]The authors contributed equally to this work.

406 ■ **ABBREVIATIONS USED**

407 ■ HSQC, heteronuclear single quantum coherence; HMBC, heteronuclear multiple

408 bond correlation.

409 ■ **REFERENCES**

410 (1) Matsuda, H.; Morikawa, T.; Ueda, H.; Yokhikawa, M. Medicinal foodstuffs.

411 XXVII. Saponin constituents of gotu kola (2): structures of new ursane- and

412 oleanane-type triterpene oligoglycosides, centellasaponins B, C, and D, from *Centella*

413 *asiatica* cultivated in Sri Lanka. *Chem. Pharm. Bull.* **2001**, *49*, 1368-1371.

414 (2) Subaraja, M.; Vanisree, A. J. The novel phytocomponent asiaticoside-D isolated

415 from *Centella asiatica* exhibits monoamine oxidase-B inhibiting potential in the

416 rotenone degenerated cerebral ganglions of *Lumbricus terrestris*. *Phytomedicine* **2019**,

417 *58*, 152833.

418 (3) Brinkhaus, B.; Lindner, M.; Schuppan, D.; Hahn, E. G. Chemical,

419 pharmacological and clinical profile of the East Asian medical plant *Centella aslatica*.

420 *Phytomedicine* **2000**, *7*, 427-448.

421 (4) Shukla, A.; Rasik, A. M.; Jain, G. K.; Shankar, R.; Kulshrestha, D. K.; Dhawan,
422 B. N. *In vitro* and *in vivo* wound healing activity of asiaticoside isolated from *Centella*
423 *asiatica*. *J. Ethnopharmacol.* **1999**, *65*, 1–11.

424 (5) Sabaragamuwa, R.; Perera, C. O.; Fedrizzi, B. *Centella asiatica* (Gotu kola) as a
425 neuroprotectant and its potential role in healthy ageing. *Trends Food Sci. Tech.* **2018**,
426 *79*, 88-97.

427 (6) Shen, X. Q.; Guo, M. M.; Yu, H. Y.; Liu, D.; Lu, Z.; Lu, Y. H.
428 Propionibacterium acnes related anti-inflammation and skin hydration activities of
429 madecassoside, a pentacyclic triterpene saponin from *Centella asiatica*. *Biosci.*
430 *Biotech. Bioch.* **2019**, *83*, 561-568.

431 (7) Kwon, K. J.; Bae, S.; Kim, K.; An, I. S.; Ahn, K. J.; An, S.; Cha, H. J.
432 Asiaticoside, a component of *Centella asiatica*, inhibits melanogenesis in B16F10
433 mouse melanoma *Mol. Med. Rep.* **2014**, *10*, 503-507.

434 (8) Gray, N. E.; Magana, A. A.; Lak, P.; Wright, K. M.; Quinn, J.; Stevens, J. F.;
435 Maier, C. S.; Soumyanath, A. *Centella asiatica*: phytochemistry and mechanisms of
436 neuroprotection and cognitive enhancement. *Phytochem. Rev.* **2018**, *17*, 161-194.

437 (9) Viswanathan, G.; Dan, V. M.; Radhakrishnan, N.; Nair, A. S.; Rajendran Nair, A.
438 P.; Baby, S. Protection of mouse brain from paracetamol-induced stress by *Centella*
439 *asiatica* methanol extract. *J. Ethnopharmacol.* **2019**, *236*, 474–483.

440 (10) He, L. L.; Hong, G. J.; Zhou, L.; Zhang, J. G.; Fang, J.; He, W.; Tickner J.;
441 Han, X. R.; Zhao, L. L.; Xu, J. K. Asiaticoside, a component of *Centella asiatica*

442 attenuates RANKL-induced osteoclastogenesis via NFATc1 and NF-κB signaling
443 pathways. *J. Cell. Physiol.* **2019**, *234*, 4267-4276.
444 (11) James, J.; Dubery, I. Identification and quantification of triterpenoid
445 centelloids in *Centella asiatica* (L.) urban by densitometric TLC. *J. Plan. Chromatogr.*
446 *Mod. TLC* **2011**, *24*, 82-87.
447 (12) Shao, Y.; Ou-Yang, D. W.; Cheng, L.; Gao, W.; Weng, X. X.; Kong, D. Y.
448 New pentacyclic triterpenoids from *Centella asiatica*. *Helv. Chim. Acta* **2015**, *98*,
449 683-690.
450 (13) Shao, Y.; Ou-Yang, D. W.; Gao, W.; Cheng, L.; Weng, X. X.; Kong, D. Y.
451 Three new pentacyclic triterpenoids from *Centella asiatica*. *Helv. Chim. Acta* **2014**,
452 *97*, 992-998.
453 (14) Nhiem, N. X.; Tai, B. H.; Quang, T. H.; Kiem, P. V.; Minh, C. V.; Nam, N. H.;
454 Kim, J. H.; Im, L. R.; Lee, Y. M.; Kim, Y. H. A new ursane-type triterpenoid
455 glycoside from *Centella asiatica* leaves modulates the production of nitric oxide and
456 secretion of TNF-α in activated RAW 264.7 cells. *Bioorg. Med. Chem. Lett.* **2011**, *21*,
457 1777-1781.
458 (15) Matsuda, H.; Morikawa, T.; Ueda, H.; Yoshikawa, M. Medicinal foodstuffs.
459 XXVI. Inhibitors of aldose reductase and new triterpene and its oligoglycoside,
460 Centellasapogenol A and Centellasaponin A, from *Centella asiatica* (Gotu kola).
461 *Heterocycles* **2001**, *55*, 1499-1504.
462 (16) Li, F.; Du, B. W.; Lu, D. F.; Wu, W. X.; Wongkrajang, K.; Wang, L.; Pu, W.
463 C.; Liu, C. L.; Liu, H. W.; Wang, M. K.; Wang, F. Flavonoid glycosides isolated from

464 *Epimedium brevicornum* and their estrogen biosynthesis-promoting effects. *Sci.*
465 *Rep.-Uk* **2017**, *7*, 1-12.
466 (17) Hu, W. C.; Wang, G. C.; Li, P. X.; Wang, Y. N.; Si, C. L.; He, J.; Long, W.;
467 Bai, Y. J.; Feng, Z. S.; Wang, X. F. Neuroprotective effects of macranthoin G from
468 *Eucommia ulmoides* against hydrogen peroxide-induced apoptosis in PC12 cells via
469 inhibiting NF-κB activation. *Chem. Biol. Interact*. **2014**, *224*, 108-116.
470 (18) Zhang, J.; Wang, Y.; Jiang, Y.; Liu, T.; Luo, Y.; Diao, E.; Cao, Y.; Chen, L.;
471 Zhang, L.; Gu, Q.; Zhou, J.; Sun, F.; Zheng, W.; Liu, J.; Li, X.; Hu, W. Enhanced
472 cytotoxic and apoptotic potential in hepatic carcinoma cells of chitosan nanoparticles
473 loaded with ginsenoside compound K. *Carbohydr. Polym*. **2018**, *198*, 537-545.
474 (19) Cheng, S. Y.; Wang, C. M.; Hsu, Y. M.; Huang, T. J.; Chou, S. C.; Lin, E. H.;
475 Chou, C. H. Oleanane-type triterpenoids from the leaves and twigs of *Fatsia*
476 *polycarpa*. *J. Nat. Prod.* **2011**, *74*, 1744-1750.
477 (20) Ahmad, V. U.; Bano, S.; Bano, N. A triterpene acid from *Nepeta hindostana*.
478 *Phytochemistry* **1986**, *25*, 1487-1488.
479 (21) Kojima, H.; Tominaga, H.; Sato, S.; Ogura, H. Pentacyclic triterpenoids from
480 *Prunella vulgaris*. *Phytochemistry* **1987**, *26*, 1107-1111.
481 (22) Maeda, C.; Ohtani, K.; Kasai, R.; Yamasaki, K.; Duc, N. M.; Nham, N. T.; Cu,
482 N. K. Q. Oleanane and ursane glycosides from *Schefflera octophylla*. *Phytochemistry*
483 **1994**, *37*, 1131-1137.
484 (23) Fukuda, Y.; Yamada, T.; Wada, S.; Sakai, K.; Matsunaga, S.; Tanaka, R.
485 Lupane and oleanane triterpenoids from the cones of *Liquidamber styraciflua*. *J. Nat.*

486 *Prod.* **2006**, *69*, 142-144.

487 (24) Sahu, N. P.; Roy, S. K.; Mahato, S. B. Spectroscopic determination of
488 structures of triterpenoid trisaccharides from *Centella asiatica*. *Phytochemistry* **1989**,
489 *28*, 2852-2854.

490 (25) Yu, L. Q.; Duan, H. Q.; Gao, W. Y.; Takaishi, Y. A new triterpene and a
491 saponin from *Centella asiatica*. *Chin. Chem. Lett.* **2007**, *18*, 62-64.

492 (26) Wen, X. X.; Zhang, J.; Gao, W.; Cheng, L.; Shao, Y.; Kong, D. Y. Two new
493 pentacyclic triterpenoids from *Centella asiatica*. *Helv. Chim. Acta* **2012**, *95*, 255-260.

494 (27) Fang, J. Y.; Tolleson, C. The role of deep brain stimulation in Parkinson's
495 disease: an overview and update on new developments. *Neuropsychiatr. Dis. Treat.*
496 **2017**, 13, 723-732.

497 (28) Lee, D. J.; Dallapiazza, R. F.; De Vloo, P.; Lozano, A. M. Current surgical
498 treatments for Parkinson's disease and potential therapeutic targets. *Neural. Regen.*
499 *Res*. **2018**, *13*, 1342-1345.

500 (29) Harischandra, D. S.; Rokad, D.; Ghaisas, S.; Verma, S.; Robertson, A.; Jin, H.;
501 Anantharam, V.; Kanthasamy, A.; Kanthasamy, A. G. Enhanced differentiation of
502 human dopaminergic neuronal cell model for preclinical translational research in
503 Parkinson's disease. *Biochim. Biophys. Acta Mol. Basis Dis.* **2019**, *4*, 165533.

504 (30) Xu, C.L.; Qu, R.; Zhang, J.; Li, L.F.; Ma, S.P. Neuroprotective effects of
505 madecassoside in early stage of Parkinson's disease induced by MPTP in rats.
506 *Fitoterapia* **2013**, *90*, 112-118.

507 (31) Zhu, J.; Yu, W.; Liu, B.; Wang, Y. T.; Shao, J. L.; Wang, J. J.; Xia, K. S.;

508 Liang, C. Z.; Fang, W. J.; Zhou, C. H.; Tao, H. M. Escin induces caspase-dependent
509 apoptosis and autophagy through the ROS/p38 MAPK signalling pathway in human
510 osteosarcoma cells *in vitro* and *in vivo*. *Cell Death Dis*. **2017**, *8*, e3113.
511 (32) Dawson, T. M.; Dawson, V. L. Excitotoxic programmed cell death involves
512 caspase-independent mechanisms. *Acute Neuronal Injury*. Springer, Cham, **2018**,
513 3-17.
514 (33) Hou, Y.; Li X.; Peng, S.; Yao, J.; Bai, F.; Fang, J. Lipoamide ameliorates
515 oxidative stress via induction of Nrf2/ARE signaling pathway in PC12 cells. *J. Agric.*
516 *Food. Chem.* **2019**, *67*, 8227-8234.
517 (34) Song, Z. L.; Bai, F.; Zhang, B.; Fang, J. Synthesis of dithiolethiones and
518 identification of potential neuroprotective agents via activation of Nrf2-driven
519 antioxidant enzymes. *J. Agric. Food. Chem*. **2020**, *68*, 2214-2231
520 (35) Angelova, P. R.; Abramov, A. Y. Functional role of mitochondrial reactive
521 oxygen species in physiology. *Free Radical Biol. Med*. **2016**, *100*, 81-85.
522 (36) Asadi, N.; Bahmani, M.; Kheradmand, A.; Rafieian-Kopaei, M. The impact of
523 oxidative stress on testicular function and the role of antioxidants in improving it: a
524 review. *J. Clin. Diagn. Res.* **2017**, *11*, IE01-IE05.
525 (37) Wang, Y.; Kuang, H.; Xue, J.; Liao, L.; Yin, F.; Zhou, X. LncRNA AB073614
526 regulates proliferation and metastasis of colorectal cancer cells via the PI3K/AKT
527 signaling pathway. *Biomed. Pharmacother.* **2017**, *93*, 1230-1237.
528 (38) Woo, S. U.; Sangai, T.; Akcakanat, A.; Chen, H.; Wei, C.; Meric-Bernstam, F.
529 Vertical inhibition of the PI3K/Akt/mTOR pathway is synergistic in breast cancer.

530 *Oncogenesis* **2017**, *6*, e385.

531 (39) Li, Y.; Ma, X.; Wang, Y.; Li, G. miR-489 inhibits proliferation, cell cycle
532 progression and induces apoptosis of glioma cells via targeting SPIN1-mediated
533 PI3K/AKT pathway. *Biomed. Pharmacother.* **2017**, *93*, 435-443.

534 (40) Yan, T.; Sun, Y.; Gong, G.; Li, Y.; Fan, K.; Wu, B.; Bi, K.; Jia, Y. The
535 neuroprotective effect of schisandrol A on 6-OHDA-induced PD mice may be related
536 to PI3K/AKT and IKK/IκBα/NF-κB pathway. *Exp. Gerontol.* **2019**, *128*, 110743.

537 (41) Cui, C.; Cui, N.; Wang, P.; Song, S.; Liang, H.; Ji, A. Neuroprotective effect
538 of sulfated polysaccharide isolated from sea cucumber *Stichopus japonicus* on
539 6-OHDA-induced death in SH-SY5Y through inhibition of MAPK and NF-κB and
540 activation of PI3K/Akt signaling pathways. *Biochem. Biophys. Res. Commun*. **2016**,
541 *470*, 375-383.

542 (42) Lien, E. C.; Dibble, C. C.; Toker A. PI3K signaling in cancer: beyond AKT.
543 *Curr. Opin. Cell Biol*. **2017**, *45*, 62-71.

544 (43) Luo, J.; Manning, B. D.; Cantley, L. C. Targeting the PI3K-Akt pathway in
545 human cancer: rationale and promise. *Cancer Cell*, **2003**, *4*, 257-262.

546 (44) Jin, X.; Di, X.; Wang, R.; Ma, H.; Tian, C.; Zhao, M.; Cong, S.; Liu, J.; Li, R.;
547 Wang, K. RBM10 inhibits cell proliferation of lung adenocarcinoma via
548 RAP1/AKT/CREB signalling pathway. *J. Cell Mol. Med.* **2019**, *23*, 3897-3904.

549 (45) Wu, X.; Liang, Y.; Jing, X.; Lin, D.; Chen, Y.; Zhou, T.; Peng, S.; Zheng, D.;
550 Zeng, Z.; Lei, M.; Huang, K.; Tao, E.. Rifampicin prevents SH-SY5Y cells from
551 rotenone-induced apoptosis via the PI3K/Akt/GSK-3β/CREB signaling pathway.

552 *Neurochem. Res*. **2018**, *43*, 886-893.

553 (46) Dalmagro, A. P.; Camargo, A.; Rodrigues, A. L. S.; Zeni, A. L. B.
554 Involvement of PI3K/Akt/GSK-3β signaling pathway in the antidepressant-like and
555 neuroprotective effects of *Morus nigra* and its major phenolic, syringic acid. *Chem.*
556 *Biol. Interact*. **2019**, *314*, 108843.

557 (47) Li, R.; Wu, Y.; Zou, S.; Wang, X.; Li, Y.; Xu, K.; Gong, F.; Liu, Y.; Wang, J.;
558 Liao, Y.; Li, X.; Xiao, J. NGF attenuates high glucose-induced ER stress, preventing
559 schwann cell apoptosis by activating the PI3K/Akt/GSK3β and ERK1/2 pathways.
560 *Neurochem. Res.* **2017**, *42*, 3005-3018.

561 (48) Kai, G. Q.; Chen, Y.; Wang, Y.; Yan, Q. H. Separation rule of oleanane and
562 ursane pentacyclic triterpenoids isomers from nature plants by coordination
563 chromatography. *J. Chromatogr. Sci.* **2014**, *52*, 532-538.

564

565

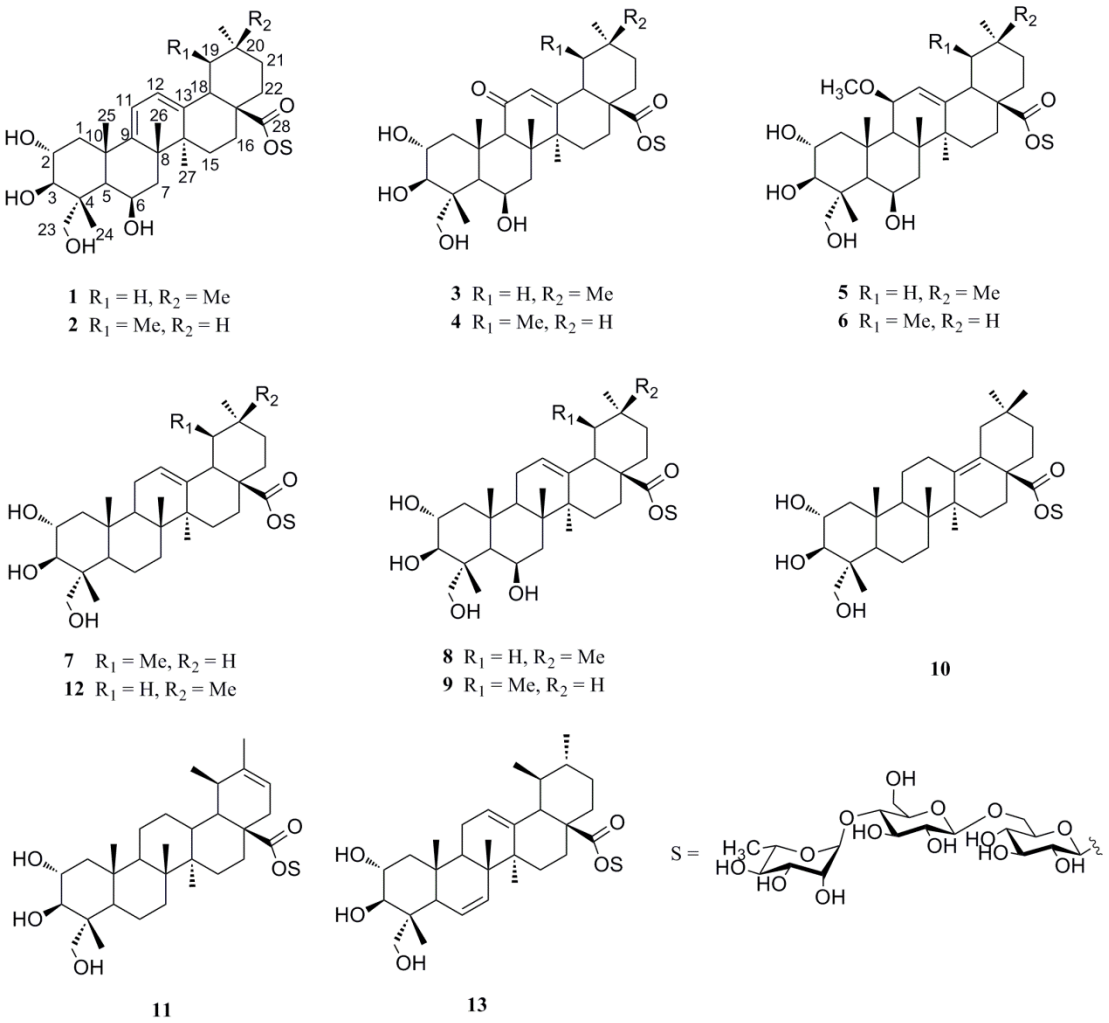

Figure 1. Compounds **1–13** isolated from *C. asiatica*.

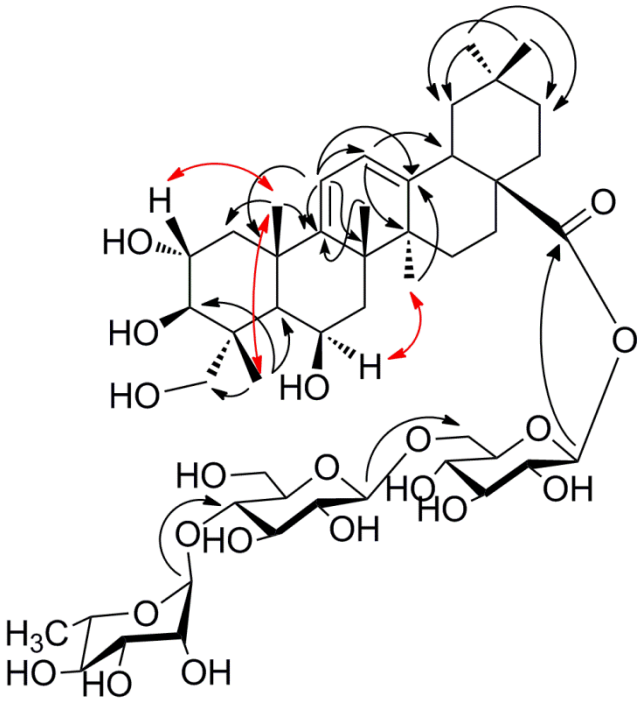

Figure 2. Key HMBC and NOE correlations of compound **1**.

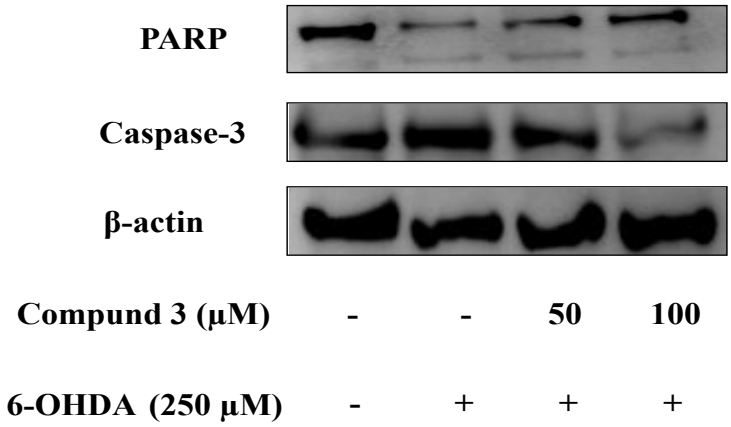

582

583 **Figure 3**. Effects of compound **3** on 6-OHDA induced cell apoptosis in PC12 cells. Cells were
584 pretreated with different concentrations of compound **3** for 30 min and then exposed to 6-OHDA
585 for 24 h. After preparation of the total protein, caspase-3 and PARP were measured by western
586 blot.

587

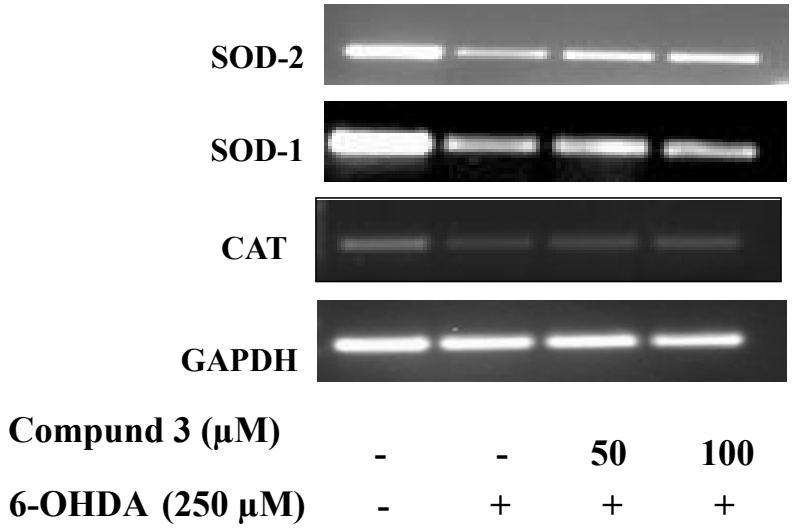

Figure 4. Effect of compound **3** on 6-OHDA induced SOD-1, SOD-1, and CAT mRNA expression. Cells were pretreated with different concentrations of compound **3** for 30 min and exposed to 6-OHDA for 24 h, and then total RNA was extracted for RT-PCR.

593

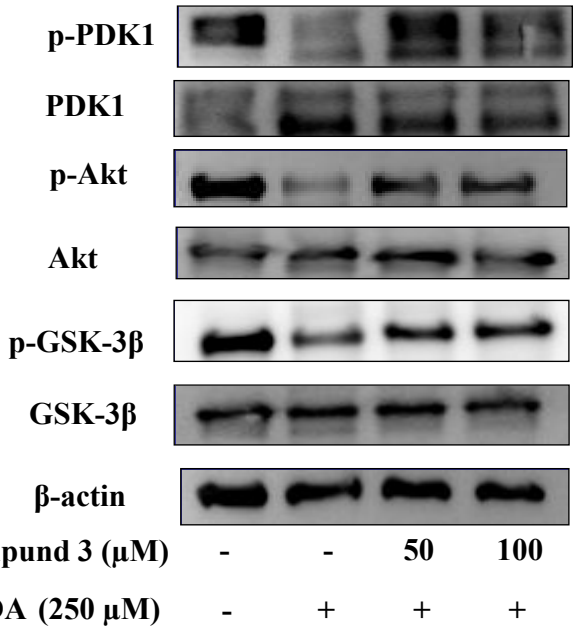

594

595 **Figure 5**. Effects of compound **3** on 6-OHDA induced PI3K/Akt/GSK-3β signaling pathway.
596 PC12 cells were pretreated with different concentrations of compound **3** for 30 min and then
597 exposed to 6-OHDA for 24 h. After preparation of the total protein, the phosphorylated and total
598 forms of PDK1, Akt, and GSK-3β were measured by western blot.

599

601 **Table 1. ^{13}C NMR data for compounds 1–6 (δ in ppm, in pyridine-d_5)[a]**

no.	1	2	3	4	5	6
aglycon						
1	48.9	49.0	50.6	50.7	51.1	51.6
2	69.8	69.1	69.2	69.0	69.3	69.3
3	78.2	78.3	78.0	78.0	78.3	78.2
4	44.5	44.4	44.8	44.9	44.7	44.7
5	45.2	45.2	48.8	48.6	49.2	49.0
6	66.8	66.7	66.9	66.8	67.7	67.6
7	40.4	40.4	40.9	41.2	41.5	41.7
8	42.0	42.0	45.0	44.8	42.9	42.6
9	155.5	155.8	63.1	62.7	53.9	53.4
10	39.9	39.0	38.8	38.6	39.5	39.4
11	121.5	123.2	200.6	199.9	76.4	77.0
12	116.4	115.9	128.7	131.5	122.9	126.3
13	145.1	139.3	169.2	162.7	148.2	141.6
14	42.5	42.8	44.8	44.9	43.0	43.2
15	27.2	28.0	28.4	29.0	28.4	28.8
16	24.2	25.2	23.4	24.5	23.5	24.7
17	46.5	47.9	45.5	48.1	46.8	48.1
18	40.2	51.6	42.3	53.3	41.4	52.7
19	46.3	39.0	31.7	38.9	46.3	39.1
20	30.8	38.8	30.9	38.9	30.8	39.1
21	33.9	30.8	34.0	30.6	34.0	30.8
22	32.4	36.7	33.0	36.0	32.5	36.8
23	66.5	66.5	65.6	65.9	66.2	66.2
24	16.1	16.0	16.1	16.1	16.1	16.1
25	30.4	30.4	20.3	20.2	20.7	20.7
26	23.0	24.0	23.8	21.2	20.2	20.5
27	20.4	18.6	20.6	20.6	25.5	23.1
28	176.8	176.5	176.5	176.1	176.6	176.4
29	33.1	17.4	33.0	17.2	33.1	17.3
30	23.7	21.5	23.6	21.2	23.7	21.3
OMe					54.3	54.5
sugars						
Glc-I						
1	95.8	95.9	96.1	96.1	95.9	95.9
2	73.8	73.8	74.0	74.1	73.9	73.8
3	78.2	78.1	78.3	78.3	78.3	78.3
4	71.0	71.1	71.0	71.1	71.0	71.1
5	78.0	78.0	78.0	78.0	78.0	78.0
6	69.8	69.2	69.3	69.5	69.3	69.5
Glc-II						
1	104.9	104.4	104.9	105.0	104.9	105.0.
2	75.5	75.5	75.4	75.4	75.4	75.4
3	76.6	76.5	76.6	76.6	76.6	76.5
4	78.6	78.6	78.5	78.5	78.6	78.6
5	77.2	77.2	77.2	77.2	77.2	77.2
6	61.3	61.3	61.5	61.4	61.3	61.4
Rha						
1	102.6	102.4	102.9	102.8	102.8	102.7
2	72.7	72.7	72.7	72.7	72.8	72.8
3	72.8	72.9	72.9	72.9	72.6	72.6
4	74.0	74.0	74.1	73.8	74.0	74.0
5	70.4	70.3	70.6	70.5	70.4	70.4
6	18.6	18.3	18.7	18.7	18.6	18.6

[a] Assignments were confirmed by HSQC, and HMBC.

602

603 **Table 2. ^{1}H NMR data for compounds 1–4 (δ in ppm, J in Hz, in pyridine-d_5)[a]**

no.	1	2	3	4	no.	1	2	3	4
aglycone					sugars				
1	1.89 (m)	1.88 (m)	1.62 (m)	1.60 (m)	Glc-I				
	2.74 (m)	2.74 (m)	3.94 (m)	3.95 (m)	1	6.18 (d, 7.5)	6.12 (d, 7.5)	6.11 (d, 8.1)	6.08 (d, 8.0)
2	4.49 (m)	4.46 (m)	4.53 (m)	4.53 (m)	2	4.32 (m)	4.36 (m)	4.30 (m)	4.30 (m)
3	3.64, d (9.4)	3.61, o	3.61, d (9.7)	3.62, d (9.5)	3	4.00 (m)	4.02 (m)	4.17 (m)	4.17 (m)
5	2.06 (m)	2.04 (m)	1.97 (m)	1.98 (m)	4	4.25 (m)	4.27 (m)	4.25 (m)	4.25 (m)
6α	5.09 (br s)	5.07 (br s)	5.09 (br s)	5.08 (br s)	5	3.58 (m)	3.61 (m)	4.30 (m)	4.27 (m)
7	1.92 (m)	1.94 (m)	1.91 (m)	1.90 (m)	6	4.28 (m)	4.25 (m)	4.25 (m)	4.26 (m)
	2.19 (m)	2.20 (m)	2.10 (m)	2.11 (m)		4.65 (m)	4.61 (m)	4.65 (m)	4.68 (m)
9			2.86 (s)	2.87 (s)	Glc-II				
11	5.75 (d, 5.2)	5.75 (d, 5.2)			1	4.96 (d, 7.0)	4.94 (d, 7.7)	4.89 (d, 7.9)	4.92 (d, 7.7)
12	6.00 (d, 5.2)	5.94 (d, 5.2)	6.00 (s)	6.02 (s)	2	3.89 (m)	3.90 (m)	3.91 (m)	3.91 (m)
15	1.22 (m)	1.22 (m)	1.24 (m)	1.25 (m)	3	4.09 (m)	4.13 (m)	3.58 (m)	3.60 (m)
	2.48 (m)	2.65 (m)	2.32 (m)	2.49 (m)	4	4.12 (m)	4.16 (m)	4.36 (m)	4.36 (m)
16	1.92 (m)	1.74 (m)	1.96 (m)	1.93 (m)	5	4.24 (m)	4.27 (m)	4.10 (m)	4.09 (m)
	1.96 (m)	1.96 (m)	1.96 (m)	2.03 (m)	6	4.02 (m)	4.07 (m)	4.03 (m)	4.04 (m)
18	3.31 (d, 10.0)	2.61 (d, 10.5)	3.18 (d, 12.0)	2.54 (d, 11.1)		4.13 (m)	4.18 (m)	4.15 (m)	4.16 (m)
19	1.21 (m)	0.84 (m)	1.28 (m)	1.35 (m)	Rha				
	1.63 (m)		1.72 (m)		1	5.83 (br s)	5.84 (br s)	5.77 (br s)	5.81 (br s)
20		1.35 (m)		0.77 (m)	2	4.66 (m)	4.70 (m)	4.65 (m)	4.62 (m)
21	1.04 (m)	1.15 (m)	1.07 (m)	1.19 (m)	3	4.53 (m)	4.55 (m)	4.51 (m)	4.51 (m)
	1.24 (m)	1.33 (m)	1.27 (m)	1.31 (m)	4	4.10 (m)	4.14 (m)	4.11 (m)	4.10 (m)
22	1.65 (m)	1.75 (m)	1.64 (m)	1.77 (m)	5	4.90 (m)	4.92 (m)	4.87 (m)	4.90 (m)
	1.82 (m)	1.90 (m)	1.80 (m)	1.88 (m)	6	1.66 (d, 5.8)	1.65 (d, 5.9)	1.65 (d, 6.1)	1.66 (d, 6.0)
23	3.99 (m)	4.03 (m)	4.06 (m)	4.04 (m)					
	4.36 (m)	4.40 (m)	4.40 (m)	4.40 (m)					
24	1.71 (s)	1.69 (s)	1.71 (s)	1.73 (s)					
25	2.04 (s)	2.04 (s)	2.13 (s)	2.19 (s)					
26	1.94 (s)	1.96 (s)	1.89 (s)	1.93 (s)					
27	1.15 (s)	1.04 (s)	1.27 (s)	1.24 (s)					
29	0.82 (s)	0.90 (d, 5.7)	0.77 (s)	0.77 (d, 6.0)					
30	0.82 (s)	0.84 (s)	0.85 (s)	0.81 (s)					

[a] Assignments were confirmed by HSQC, and HMBC. m: multiple signal.

604

605

606

607

608 **Table 3. ^{1}H NMR data for compounds 5–6 (δ in ppm, J in Hz, in pyridine-d_5)[a]**

no.	5	6	no.	5	6
aglycone			sugars		
1	1.85 (m)	1.86 (m)	Glc-1		
	2.75 (d, 9.5)	2.86 (d, 9.7)	1	6.18 (d, 7.5)	6.16 (d, 8.0)
2	4.46 (m)	4.47 (m)	2	4.30 (m)	4.32 (m)
3	3.62, d (8.2)	3.62, o	3	4.08 (m)	4.11 (m)
5	2.01 (br s)	2.04 (br s)	4	4.22 (m)	4.24 (m)
6α	5.08 (br s)	5.09 (br s)	5	3.59 (m)	3.58 (m)
7	1.86 (m)	1.78 (m)	6	4.29 (m)	4.29 (m)
	1.92 (m)	1.91 (m)		4.66 (m)	4.66 (m)
9	2.25 (d, 8.2)	2.21 (d, 8.5)	Glc-2		
11	4.13 (m)	4.21 (m)	1	4.97 (d, 7.7)	4.97 (d, 7.5)
12	5.48 (br s)	5.76 (br s)	2	3.92 (m)	3.95 (m)
15	1.11 (m)	1.11 (m)	3	4.04 (m)	4.05 (m)
	2.32 (m)	2.45 (m)	4	4.37 (m)	4.37 (m)
16	1.90 (m)	1.95 (m)	5	4.16 (m)	4.18 (m)
	2.03 (m)	2.03 (m)	6	4.07 (m)	4.08 (m)
18	3.26 (d, 13.8)	2.56 (d, 11.0)		4.18 (m)	4.21 (m)
19	2.01 (m)	1.37 (m)	Rha		
	2.10 (m)		1	5.79 (br s)	5.84 (br s)
20		0.87 (m)	2	4.67 (m)	4.71 (m)
21	1.73 (m)	1.25 (m)	3	4.67 (m)	4.68 (m)
	1.85 (m)	1.37 (m)	4	4.15 (m)	4.14 (m)
22	1.63 (m)	1.78 (m)	5	4.93 (m)	4.94 (m)
	1.81 (m)	1.90 (m)	6	1.68 (d, 6.0)	1.69 (d, 6.0)
23	4.07 (m)	4.08 (m)			
	4.41 (m)	4.42 (m)			
24	1.75 (s)	1.78 (s)			
25	1.89 (s)	1.94 (s)			
26	1.75 (s)	1.79 (s)			
27	1.27 (s)	1.18 (s)			
29	0.89 (s)	1.00 (d, 6.0)			
30	0.84 (s)	0.88 (s)			
OMe	3.30 (s)	3.31 (s)			

[a] Assignments were confirmed by HSQC, and HMBC. m: multiple signal.

609

610

611

612

613 **Table 4. Primer sequences and conditions for RT-PCR**

Genename	Primer Sequence (5'-3')
GAPDH	F: CACTCACGGCAAATTCAACGGCA R: GACTCCACGACATACTCAGCAC
SOD-1	F: CCATCAATATGGGGACAATACAC R: ACACGATCTTCAATGGACAC
SOD-2	F: TGACCTGCCTTACGACTATG R: CGACCTTGCTCCTTATTGAA
Cat	F: CAAGCTGGTTAATGCGAATGG R: TTGAAAAGATCTCGGAGGCC

614

615

616

617

618

619

620

621

622

623

624

625

626

627

628

629

630

631 **Table 5. The neuroprotective effects of triterpene saponins from *C. asiatica***

Sample	Cell viability (% of control)
Control	100±7.26[a]
6-OHDA	59.04±15.93[f]
1	57.85±2.84[f]
2	73.14±11.77[bcdef]
3	91.75±7.06[ab]
4	78.18±7.17[bcde]
5	69.53±0.66[cdef]
6	62.09±6.96[def]
7	84.02±6.07[abc]
8	87.97±10.96[abc]
9	81.04±3.88[bcd]
10	69.09±7.90[cdef]
11	86.84±4.03[abc]
12	71.61±15.75[cdef]
13	73.11±4.52[cdef]

The data are presented as means ± SD (n = 3). Values with the same superscript letters are not significantly different from each other at $p < 0.05$

632

633

634

635

636

637

638

639

640

641

642

643

644 Table of Contents

645 Zhou-Wei Wu[†,§], Wei-Bo Li[‡,§], Jing Zhou[‡], Xin Liu[∥], Lun Wang[†], Bin Chen[†],

646 Ming-Kui Wang[†], Lilian Ji[‡], Wei-Cheng Hu*[,‡], and Fu Li*[,†]

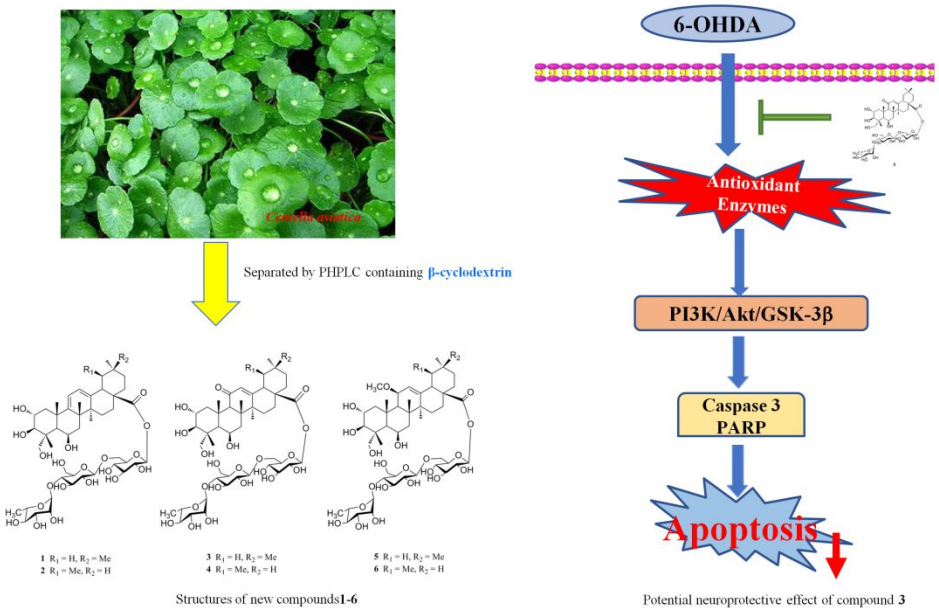

647 Structures of new compounds **1-6** Potential neuroprotective effect of compound **3**